Available online at www.sciencedirect.com
ScienceDirect
Carbohydrate Polymers 68 (2007) 235–241
Carbohydrate Polymers
www.elsevier.com/locate/carbpol

Studying cellulose fiber structure by SEM, XRD, NMR and acid hydrolysis

Haibo Zhao, Ja Hun Kwak, Z. Conrad Zhang, Heather M. Brown, Bruce W. Arey, Johnathan E. Holladay *

Institute for Interfacial Catalysis, Pacific Northwest National Laboratory, P.O. Box 999, Richland, WA 99352, USA

Received 9 June 2006; received in revised form 12 December 2006; accepted 14 December 2006
Available online 22 December 2006

Abstract

Cotton linters were partially hydrolyzed in dilute acid and the morphology of remaining macrofibrils was studied with scanning electron microscopy (SEM) under various magnifications. The crystalline region in cellulose is composed of microfibril bundles instead of separated microfibrils. These microfibril bundles in the macrofibrils were exposed by removing amorphous cellulose on and near the surface of the macrofibers. XRD suggests that the microfibril bundles have diameters of 20–30 nm. Cellulose apparent crystallinity was not altered by hydrolysis, as indicated by XRD and NMR results. These facts suggest that amorphous cellulose in the bulk (not on the surface) is not accessible to hydrolysis and that microfibril bundles are hydrolyzed through a surface reaction process. The observed agglomerization of macrofibers could be the result of the high surface potential from the remaining microfibrils or acid catalyzed intermolecular surface dehydration between macrofibrils.

Keywords: Cellulose; Cotton linter; Macrofibril; Microfibril; Hydrolysis; SEM; XRD; NMR; Amorphous

1. Introduction

Cellulose, the most abundant renewable polymer available, is produced by nature at an annual rate of 10^{11}–10^{12} tons (Hon, 1994). If cellulose can be efficiently converted to monomeric sugars by hydrolytic processes, it can better compete with starch and play an important role to meet future energy needs. Hydrolytic processes are also used to remove amorphous cellulose in forming cellulose nanocrystals (Ranby, 1951). Cellulose nanocrystals have received increasing interest due to their natural, renewable origins and good mechanical properties (Podsiadlo et al., 2005). For example, cellulose nanocrystals are very attractive in making low cost, lightweight, and high-strength hybrid composites for multiple applications (Samir, Alloin, & Dufresne, 2005). Regardless of ones purpose for doing hydrolysis, a more fundamental understanding of the hydrolysis process would lead to improved methods for preparing cellulose for conversion into fuels or materials.

Cellulose is a polymer consisting of unbranched $\beta(1 \rightarrow 4)$ D-glucopyranosyl units. The cellulose chains have a strong tendency to aggregate to highly ordered structural entities due to their chemical constitution and spatial conformation. An understanding of the crystalline region was greatly expanded by the work of Nishiyama et al. using X-ray neutron fiber diffraction in which they were able to identify the hydrogen bonding network of I_α and I_β cellulose, the two naturally occurring crystal phases (Nishiyama, Sugiyama, Chanzy, & Langan, 2003). In addition to the crystalline regions (highly ordered), cellulose also contains amorphous regions. Hearle (1958) proposed a two-phase model with regions of high order and regions of low order. More recent models employ architectures of fibrillar units. Common structure schemes include skin

* Corresponding author. Tel.: +1 509 375 2025; fax: +1 509 372 4732.
E-mail address: john.holladay@pnl.gov (J.E. Holladay).

0144-8617/$ - see front matter © 2007 Elsevier Ltd. All rights reserved.
doi:10.1016/j.carbpol.2006.12.013

and core networks. Crystallinity of the skin and core has been examined. In one study, Müller et al., compared the crystallinity differences in the skin and core of cellulose viscose fiber by X-ray microbeam and electron diffraction mapping. They found that the crystallinity of the skin and the core were the same but that the skin contained both voids and highly oriented microfibers whereas the strands in the core were less oriented. Differences observed in the two regions were not due to changes or size of the crystalline areas (Müller, Riekel, Vuong, & Chanzy, 2000). More commonly, morphology has been studied using microscopy techniques, such as scanning electron microscopy (SEM), atomic force microscopy (AFM), transmission electron microscopy (TEM), and chemical force microscopy (CFM) (Bastidas et al., 2005, Hanley, Giasson, Revol, & Gray, 1992). One interesting outcome of morphological studies has been an understanding of how fibril strands tend to twist and can form chiral helixes. AFM work has shown that the handedness of the twist is not random but appears to be a response to the chiral nature of glucose (Hanley, Revol, Godbout, & Gray, 1997).

Morphological studies to date have looked at natural and model cellulose. We are interested in understanding how morphology changes after differing amounts of hydrolysis have occurred. In this paper, SEM, X-ray diffraction (XRD), and cross polarization/magic angle spinning (CP/MAS) ^{13}C solid-state NMR were used to follow the structural changes in cellulose cotton linterns, one form of natural cellulose, after various levels of hydrolysis. We directly observed and measured the crystallinity in cellulose (XRD and NMR) and compared those results with morphology changes observed by SEM. Cotton linters have a relatively high degree of crystallinity (56–63%) (Fink & Walenta, 1994). The highly ordered structural entities in cotton linters, called microfibrils, are the smallest well-defined morphological entities. A cotton linter fiber composed of crystalline and non-crystalline (amorphous) regions can also be called a macrofibril. It has been proposed that microfibrils can aggregate to larger morphological entities with diameters in the range of 10–50 nm (Fink, Hofmann, & Purz, 1990). This aggregation may lead to the formation of crystalline regions in cellulose, but these regions have not yet been completely separated and measured. SEM cannot distinguish amorphous from crystalline regions in the same fiber of cellulose. However, examining the morphology before and after hydrolysis may help explicate the hydrolysis process. The hydrolysis rate of the amorphous region is much higher than that of the crystalline region in cellulose (Zhao et al., 2006). Under controlled conditions, hydrolysis may remove the amorphous region of the cellulose fiber and leave the crystalline region almost untouched (Samir et al., 2005). SEM studies of acid hydrolysis can not only measure the dimensions of residual cellulose crystals, but also provide important data about the formation of cellulose nanocrystals.

2. Materials and methods

2.1. Cellulose hydrolysis and sample preparation

Cellulose (cotton linters) was directly purchased from Sigma–Aldrich (Product No. C6663). Hydrolysis tests were all done in a single experiment under identical conditions employing a Symyx heated orbital shaker reactor system (HOSS) with a six well plate; reactants (0.5 g cellulose and 7.5 g of sulfuric acid solution with concentration of 0.1, 0.2 and 0.4 M) were sealed in vials fixed on an aluminum plate and placed in a high pressure reactor (HiP) on the HOSS. The reactor, pressurized with 100 psi N_2, was heated to 150 °C and the reactants shaken at 600 rpm. After 30 min, the reactor was quenched immediately in a cold water bath. One additional experiment was done, employing 0.1 M sulfuric acid and 10 min reaction time but keeping other conditions the same. Products were treated under identical conditions. Upon filtering, the liquid products in vials were analyzed by high-pressure liquid chromatography (HPLC) using a Bio-Rad Aminex HPX-87H column and a refractive index detector. The solid products were fully rinsed by D.I. water and dried at room temperature under house vacuum for 4 h. The solids were studied by SEM and XRD.

2.2. Scanning electron microscopy (SEM)

A Zeiss-LEO 982 Scanning Electron Microscopy operated at 2 keV was used to image cellulose samples after hydrolysis. Samples were coated with carbon using a vacuum sputter-coater to improve the conductivity of the samples and thus the quality of the SEM images.

2.3. X-ray diffraction method (XRD)

XRD measurements were performed on a Philips PW3040/00 X'Pert MPD system. The diffracted intensity of Cu Kα radiation ($\lambda = 0.1542$ nm; 50 kV and 40 mA) was measured in a 2θ range between 10° and 50°.

2.4. ^{13}C solid state NMR

Cross polarization/magic angle spinning (CP/MAS) ^{13}C solid-state NMR experiments were performed on a Chemagnetics CMX100 spectrometer operating under a static field strength of 2.3 T (100 mHz ^1H) at 25 °C. The contact time for CP was 1 ms with a proton 90° pulse of 5.5 μs and decoupling power of 45 kHz. The MAS speed was 3 kHz. The delay time after the acquisition of the FID signal was 2 s. The chemical shifts were calibrated by using an external hexamethylbenzene standard methyl resonance at 17.3 ppm.

3. Results and discussions

HPLC results show that glucose was the dominant soluble material in products. Very small amounts of levulinic

acid and 5-hydroxymethyl-2-furfuraldehyde (HMF) were also detected. Calculated from glucose, levulinic acid, and HMF yields, the cellulose conversion was 5.3%, 11.8%, and 25.5% when 0.1, 0.2, and 0.4 M sulfuric acid were used. When 0.1 M sulfuric acid and 10 min reaction time were employed, 1.0% cellulose conversion was obtained.

Figs. 1a–c are SEM images of untreated cotton linters under various magnifications. Fig. 1a clearly shows the shape and size distribution of the macrofibrils in cotton linters. These well-separated macrofibrils have lengths of 300–500 μm and diameters of 10–20 μm. The SEM images (Fig. 1b and c) of one individual macrofibril at larger magnification show that the surface of untreated cotton linters is almost free of trenches, but there are obvious boundary edges in different regions. After 1.0% of cotton linters were hydrolyzed to sugar monomers. SEM images were taken of the cotton linters (Figs. 2a–c). Fig. 2a shows that the macrofibrils are still well separated and their diameters are almost the same, but the lengths of macrofibrils dropped slightly. Fig. 2b shows one individual macrofibril. In this figure, significant changes on the surface are obvious as the surface cover on cotton linters was removed. A closer look at the macrofibril surface (Fig. 2c) at larger magnification shows that many terraces, steps, and kinks form after minimal hydrolysis. The light lines on Fig. 2b are the steps formed in hydrolysis. We propose that these changes result from the removal of very reactive amorphous cellulose on the surface.

Figs. 3a–c show SEM images of cotton linters that were hydrolyzed more thoroughly, with conversion of 5.3% to sugar monomers. Fig. 3a shows that some macrofibrils remain separated, but other macrofibrils agglomerate. The agglomeration prevents us from correctly measuring the length and diameter of corresponding macrofibrils. Thus, the changes of macrofibrils in length and diameter were unable to be followed statistically in hydrolysis once the macrofibrils starts to agglomerate. The terraces, steps, and kinks seen in Figs. 2b and c disappear in Figs. 3b and c, where now numerous dots 20–30 nm in diameter are apparent. Certainly, the dots observed in Figs. 3b and c are not the ends of microfibrils, but are larger morphological entities (Fink et al., 1990). The reported diameter of microfibrils in cotton linters is 7–9 nm (Fink et al., 1990), and is confirmed by our X-ray diffraction experiments (described below). These morphological entities, called microfibril bundles in the rest of this paper, were observed only when the amorphous cellulose near the surface of the macrofibril was removed by hydrolysis.

At a cellulose conversion of 11.8%, the agglomeration of macrofibrils was greatly increased, as shown in Fig. 4a. Even though we cannot precisely measure the length of the macrofibrils, they are clearly shortened. Figs. 4b and c show the morphology of one individual macrofibril when 11.8% of cellulose was converted to sugar monomers: bundles formed from the aggregation of microfibrils are further exposed. The exposed parts are much like rods, with diameter of 20–30 nm. The ends of these rods correspond to the dots observed in Figs. 3b and c. At further conversion to 25.5% the remaining macrofibrils have agglomerated even more (Fig. 5a). The rod structure of microfibril bundles becomes clearer in Figs. 5b and c than at lower levels of conversion; however, their diameters remain roughly the same, between 20 and 30 nm.

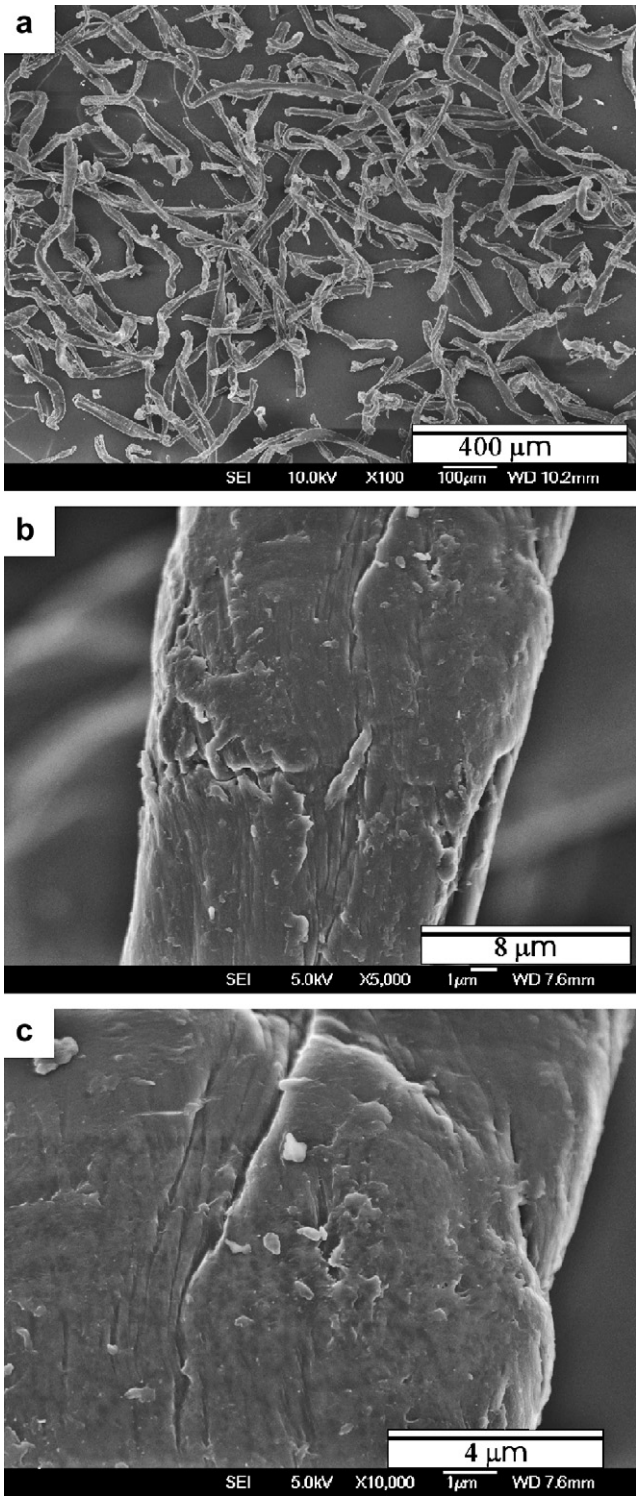

Fig. 1. Untreated cotton linters: SEM images under different magnifications (a) 100× (b) 5000× and (c) 10000×.

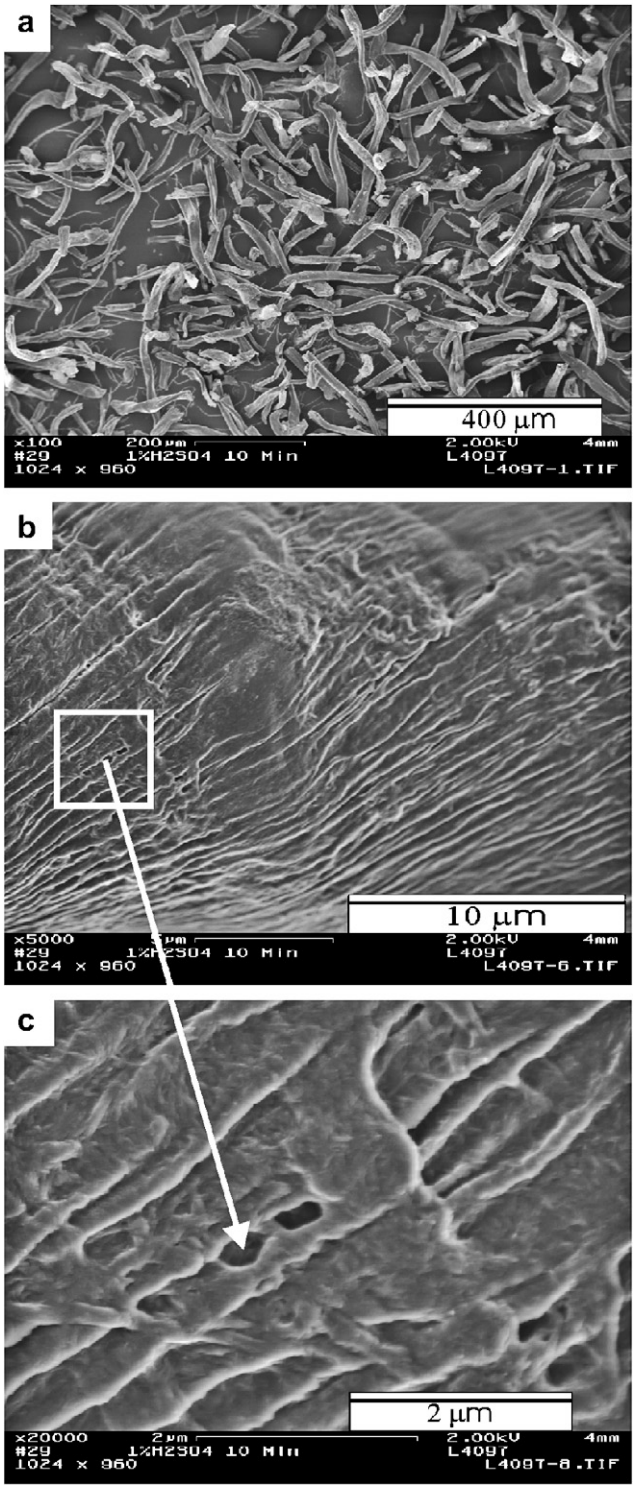

Fig. 2. Cotton linters after 1.0% cellulose was hydrolyzed: SEM images under different magnifications (a) 100× (b) 5000× (c) 20000×. The rectangle on (b) represents a typical area zoomed on (c).

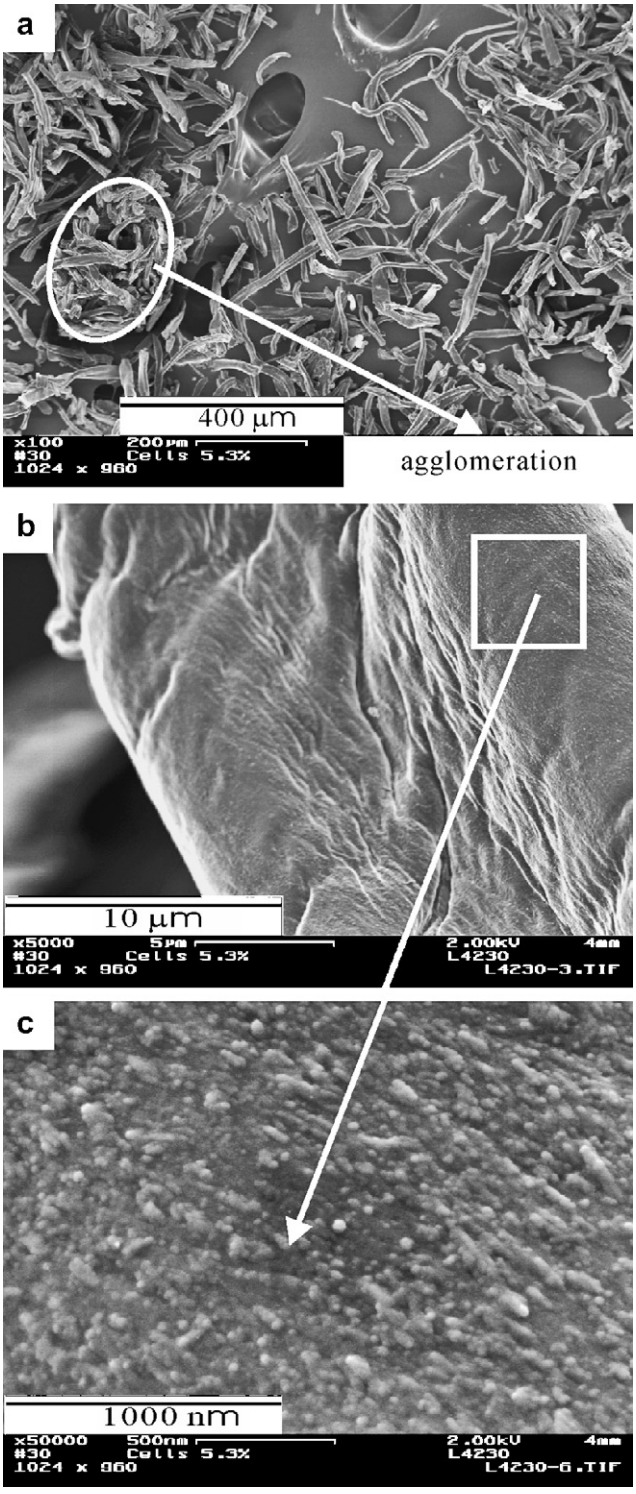

Fig. 3. Cotton linters after 5.3% cellulose was hydrolyzed: SEM images under different magnification (a) 100× (b) 5000× (c) 50000×. The rectangle on (b) represents a typical area zoomed on (c).

Although dramatic morphology changes on cellulose macrofibrils were observed at increased hydrolysis levels, no change in the XRD patterns and NMR data are were detected, as shown in Figs. 6 and 7. The XRD patterns shows that the ordered structure of the crystalline region on the remaining cellulose is not disrupted by hydrolysis. Based on the line width of the peak from crystalline plane 002 and using the Scherrer Equation, we estimate the lateral dimension of the microfibrils in untreated cotton linters at 7.3 nm (Murdock, 1930). This lateral dimension did not change during hydrolysis. The XRD data also indicates that the crystallinity of cellulose after hydrolysis does

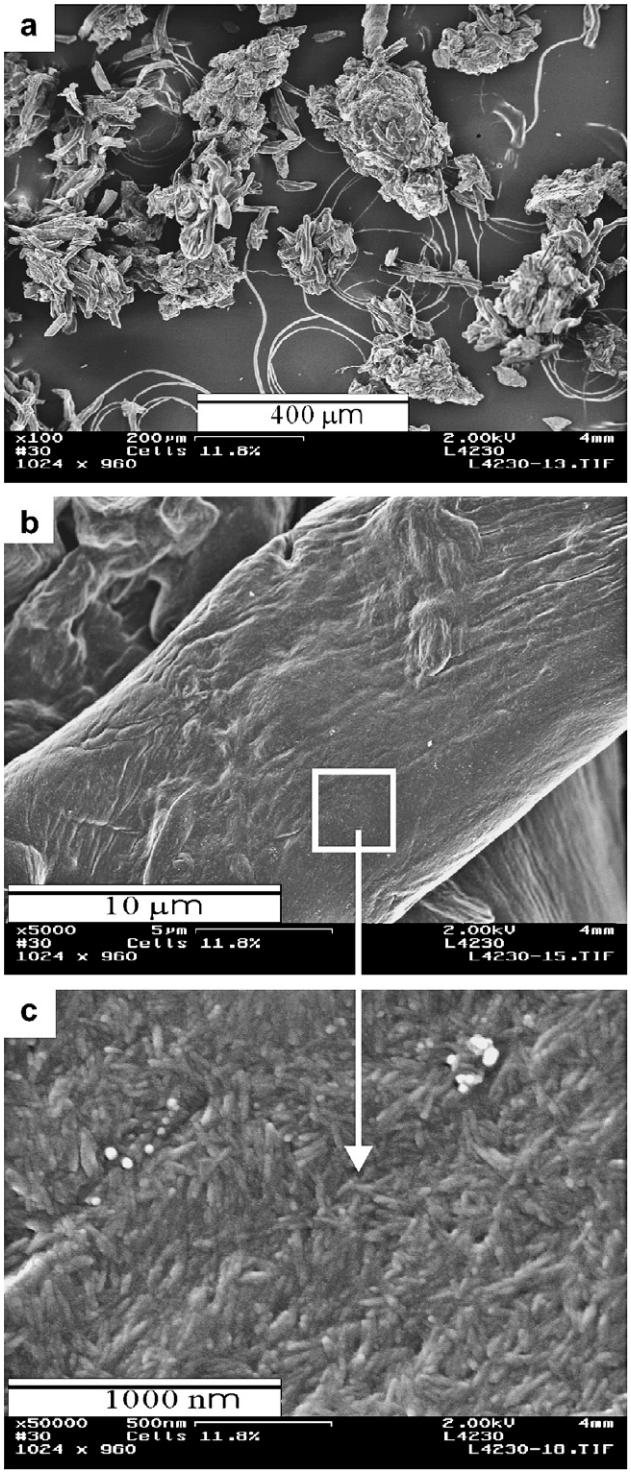

Fig. 4. Cotton linters after 11.8% cellulose was hydrolyzed: SEM images under different magnification (a) 100× (b) 5000× (c) 50000×. The rectangle on (b) represents a typical area zoomed on (c).

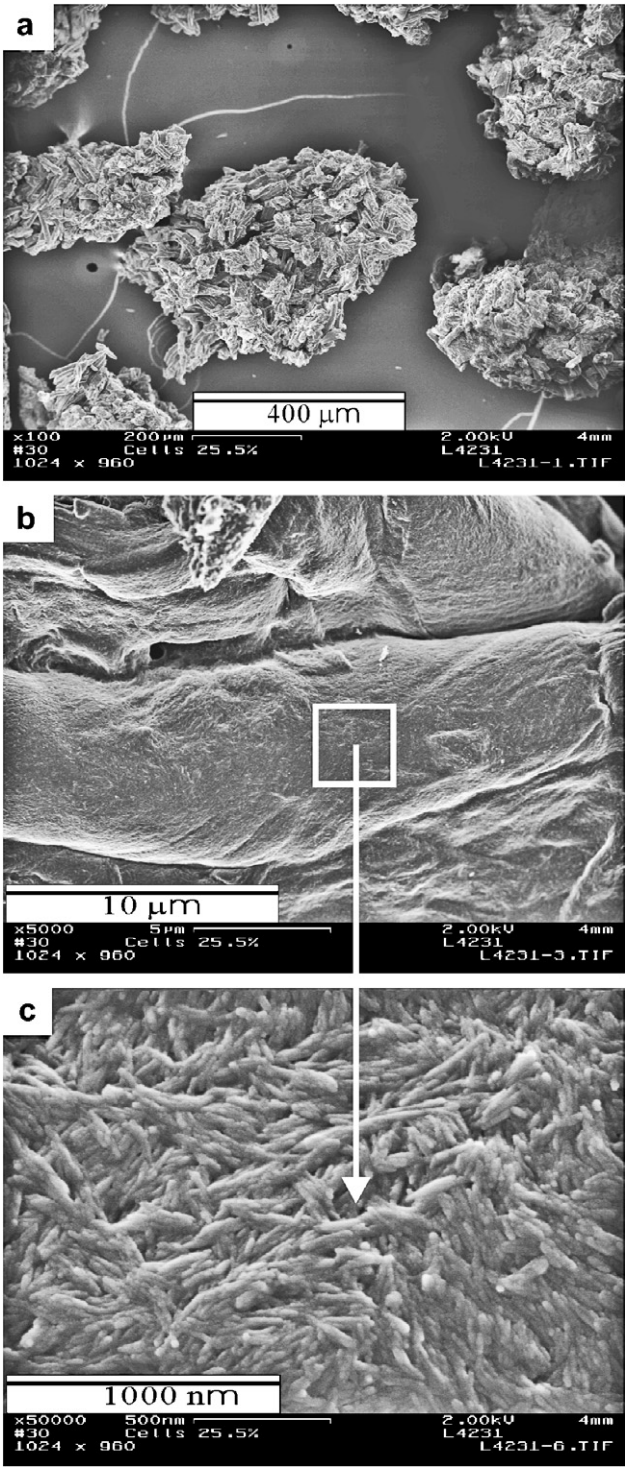

Fig. 5. Cotton linters after 25.5% cellulose was hydrolyzed: SEM images under different magnification (a) 100× (b) 5000× (c) 50000×. The rectangle on (b) represents a typical area zoomed on (c).

not increase although it is well known that amorphous cellulose is more reactive. NMR data are consistent with this finding; the peak ratio of $C4_{(79–86ppm)}/C4_{(86–92ppm)}$ in Fig. 7, which is often used to estimate the cellulose crystallinity (Liitiä et al., 2003), remains the same after hydrolysis. This fact means the relative ratio of amorphous cellulose and crystalline cellulose was not significantly changed by hydrolysis.

The large difference in reactivity between amorphous and crystalline cellulose results in the fast removal of amorphous cellulose near the macrofibrils' surface, which leads to the exposure of microfibril bundles. However, the quick

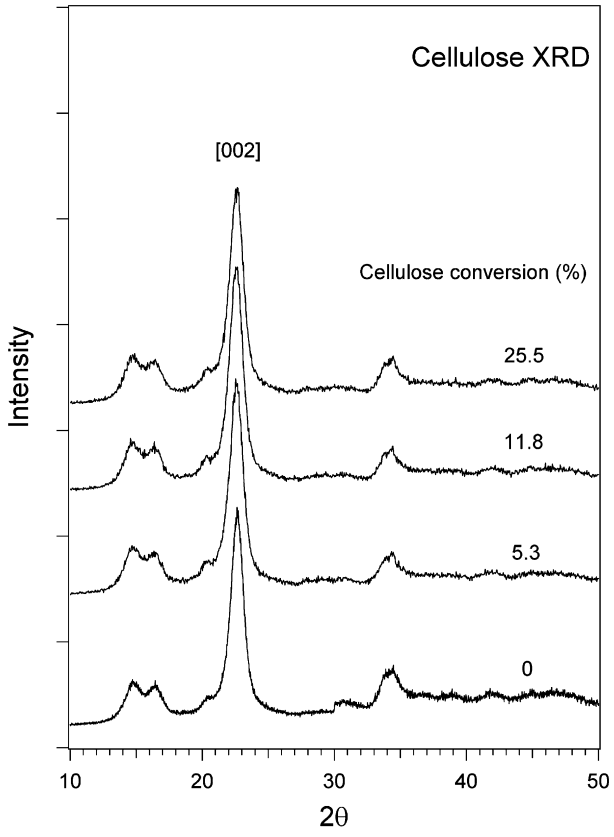

Fig. 6. XRD patterns of untreated cotton linters and partially hydrolyzed with cellulose conversion of 5.3%, 11.8%, and 25.5% as indicated.

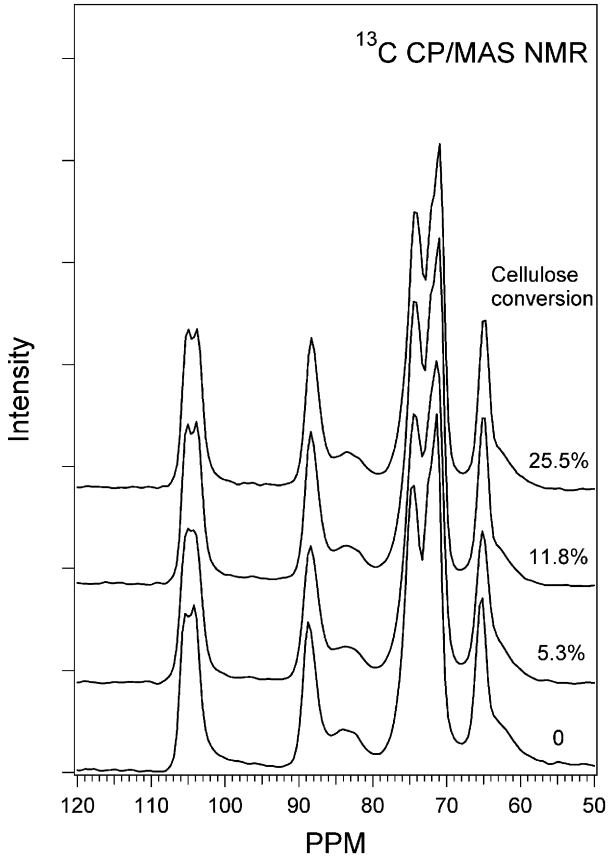

Fig. 7. (CP/MAS) ^{13}C solid-state NMR spectra of untreated cotton linters and partially hydrolyzed with cellulose conversion of 5.3%, 11.8%, and 25.5% as indicated.

loss of this surface amorphous cellulose does not significantly change the apparent cellulose crystallinity since the amount is very small in comparison with the amorphous cellulose in the bulk. Microfibril bundles have relatively slow hydrolysis rates. This suggests acid and water molecules are unable to penetrate into these microfibril bundles under our reaction conditions and that these microfibril bundles must be hydrolyzed through surface reaction processes. The amorphous cellulose deeply buried in the bulk leach out from macrofibrils during hydrolysis at slower rates due to barriers caused by the microfibril bundles. Thus, amorphous cellulose near surface is hydrolyzed first and followed by crystalline cellulose near surface. This process repeats during the hydrolysis process until cellulose degradation occurs.

The fringe fibrillar model proposed by Hearle (1958) is an appropriate and well accepted model to explain cellulose structure at the border between the supramolecular and morphological levels. This model suggests that microfibrils are the smallest basic fibril structural units surrounded by amorphous cellulose. Our SEM experimental results suggest that microfibrils exist in cotton linters as bundles and it is these microfibril bundles, surrounded by amorphous cellulose, that form macrofibrils.

When cellulose was dried at room temperature under vacuum, we observed higher levels of macrofibril agglomeration at higher levels of hydrolysis. After macrofibrils were hydrolyzed and rinsed, the volume of amorphous cellulose was occupied by water molecules that were then removed under vacuum; the remaining macrofibrils contain large amounts of naked microfibril bundles. The observed agglomerization of macrofibers could be the result of the high surface potential from the remaining microfibrils. However, we observed that agglomerization was proportional to acid strength. This suggests that agglomerization could also be the result of acid catalyzed intermolecular surface dehydration between macrofibrils.

4. Conclusions

Amorphous cellulose near the surface of macrofibrils was hydrolyzed readily, exposing microfibril bundles (with diameter 20–30 nm) in the macrofibrils, as directly observed in SEM. XRD experiments confirm that the lateral dimension of microfibrils in cotton linters remains at 7.3 nm after hydrolysis. The data suggest that microfibril bundles, rather than separated microfibrils, form the crystalline region in cellulose. Since these microfibril bundles cannot be penetrated by acid and water molecules, they are hydrolyzed through a surface reaction process. XRD and NMR results show that cellulose apparent crystallinity was not alternated by hydrolysis, which suggests that the

leaching of amorphous cellulose in the bulk should be very slow. When the macrofibrils lose amorphous cellulose, the remaining microfibril bundles have large surface potential, which could drive the agglomeration of macrofibrils to lower the system energy; alternatively, acid catalyzed intermolecular surface dehydration could also result in agglomerization.

Acknowledgements

This work was supported by the Laboratory Directed Research and Development Program at the Pacific Northwest National Laboratory (PNNL), a multiprogram national laboratory operated by Battelle for the U.S. Department of Energy under Contract DE-AC06-76RL01830. Part of the research described in this paper was performed at the Environmental Molecular Science Laboratory, a national scientific user facility located at PNNL.

References

Bastidas, J., Venditti, R., Pawlak, J., Glibert, R., Zauscher, S., & Kadla, J. F. (2005). Chemical force microscopy of cellulosic fibers. *Carbohydrate Polymers, 62*, 369–378.

Fink, H. P., Hofmann, D., & Purz, H. J. (1990). On the fibrillar structure of native cellulose. *Acta Polymerica, 41*, 131–137.

Fink, H. P., & Walenta, E. (1994). X-ray-diffraction investigations of cellulose supramolecular structure at processing. *Papier (Darmstadt), 48*, 739–748.

Hanley, S. J., Giasson, J., Revol, J.-F., & Gray, D. G. (1992). Atomic force microscopy of cellulose microfibrils: comparison with transmission electron microscopy. *Polymer, 33*, 4639–4642.

Hanley, S. J., Revol, J.-F., Godbout, L., & Gray, D. G. (1997). Atomic force microscopy and transmission electron microscopy of cellulose from *Micrasterias deniticulata*; evidence for a chiral helical microfibril twist. *Cellulose, 4*, 209–220.

Hearle, J. W. S. (1958). A fringed fibril theory of structure in crystalline polymers. *Journal of Polymer Science, 28*, 432–435.

Hon, D. N. S. (1994). Cellulose: a random walk along its historical path. *Cellulose, 1*(1), 1–25.

Liitiä, T., Maunu, S. L., Hortling, B., Tamminen, T., Pekkala, O., & Varhimo, A. (2003). Cellulose crystallinity and ordering of hemicelluloses in pine and birch pulps as revealed by solid-state NMR spectroscopic methods. *Cellulose, 10*, 307–316.

Müller, M., Riekel, C., Vuong, R., & Chanzy, H. (2000). Skin/core microstructure in viscose rayon fibres analysed by X-ray microbeam and electron diffraction mapping. *Polymer, 41*, 2627–2632.

Murdock, C. C. (1930). The form of the X-ray diffraction bands for regular crystals of colloidal size. *Physical Review, 35*, 8–23.

Nishiyama, Y., Sugiyama, J., Chanzy, H., & Langan, P. (2003). Crystal structure and hydrogen bonding system in cellulose I_α from synchrotron X-ray and neutron fiber diffraction. *J. Am. Chem. Soc., 125*, 14300–14306.

Podsiadlo, P., Choi, S. Y., Shim, B., Lee, J., Cuddihy, M., & Kotov, N. A. (2005). Molecularly engineered nanocomposites: layer-by-layer assembly of cellulose nanocrystals. *Biomacromolecules, 6*, 2914–2918.

Ranby, B. G. (1951). The colloidal properties of cellulose micelles. *Discussions of the Faraday Society, 11*, 158–164.

Samir, M. A. S. A., Alloin, F., & Dufresne, A. (2005). Review of recent research into cellulosic whiskers, their properties and their application in nanocomposite field. *Biomacromolecules, 6*, 612–626.

Zhao, H., Kwak, J. H., Wang, Y., Franz, J. A., White, J. M., & Holladay, J. H. (2006). Effects of crystallinity on dilute acid hydrolysis of cellulose by cellulose ball-milling study. *Energy & Fuels, 20*, 807–811.